

Theoretical study on the transition properties of AlF

Yun-Guang Zhang(张云光), Ling-Ling Ji(吉玲玲), Ru Cai(蔡茹),Cong-Ying Zhang(张聪颖), and Jian-Gang Xu(徐建刚)

Citation: Chin. Phys. B, 2022, 31 (**5**): 053101. DOI: 10.1088/1674-1056/ac3648
Journal homepage: http://cpb.iphy.ac.cn; http://iopscience.iop.org/cpb

What follows is a list of articles you may be interested in

Highly accurate theoretical study on spectroscopic properties of SH including spin-orbit coupling

Shu-Tao Zhao(赵书涛), Xin-Peng Liu(刘鑫鹏), Rui Li(李瑞), Hui-Jie Guo(国慧杰), and Bing Yan(闫冰)
Chin. Phys. B, 2021, 30 (**7**): 073104. DOI: 10.1088/1674-1056/ac003f

Configuration interaction study on low-lying states of AlCl molecule

Xiao-Ying Ren(任笑影), Zhi-Yu Xiao(肖志宇), Yong Liu(刘勇), and Bing Yan(闫冰)
Chin. Phys. B, 2021, 30 (**5**): 053101. DOI: 10.1088/1674-1056/abd46a

Theoretical insights into photochemical ESITP process for novel DMP-HBT-py compound

Guang Yang(杨光)†, Kaifeng Chen(陈凯锋), Gang Wang(王岗), and Dapeng Yang(杨大鹏)
Chin. Phys. B, 2020, 29 (**10**): 103103. DOI: 10.1088/1674-1056/aba9bb

Exploration and elaboration of photo-induced proton transfer dynamical mechanism for novel 2-[1,3]dithian-2-yl-6-(7aH-indol-2-yl)-phenol sensor

Lei Xu(许磊), Tian-Jie Zhang(张天杰), Qiao-Li Zhang(张巧丽), Da-Peng Yang(杨大鹏)
Chin. Phys. B, 2020, 29 (**5**): 053102. DOI: 10.1088/1674-1056/ab8208

Vibronic spectra of aluminium monochloride relevant to circumstellar molecule

Jian-Gang Xu(徐建刚), Cong-Ying Zhang(张聪颖), Yun-Guang Zhang(张云光)
Chin. Phys. B, 2020, 29 (**3**): 033102. DOI: 10.1088/1674-1056/ab6c46

Theoretical study on the transition properties of AlF

Yun-Guang Zhang(张云光)[†], Ling-Ling Ji(吉玲玲), Ru Cai(蔡茹), Cong-Ying Zhang(张聪颖), and Jian-Gang Xu(徐建刚)[‡]

School of Science, Xi'an University of Posts and Telecommunications, Xi'an 710121, *China*

(Received 5 August 2021; revised manuscript received 2 November 2021; accepted manuscript online 4 November 2021)

Potential energy curves of the $X^1\Sigma^+$ and $A^1\Pi$ states of the AlF molecule are studied through the combination of the multi-reference configuration interaction (MRCI) approach and Davidson corrections (MRCI+Q). The AWCV5Z basis set is employed in the calculations. The transition dipole moments (TDMs) of the $A^1\Pi \leftrightarrow X^1\Sigma^+$ transition are explored based on the AWCV5Z basis set and (4, 2, 2, 0) active space. The Schrödinger equation is solved via the LEVEL 8.2 program, and the vibrational levels and rotational constants of the $X^1\Sigma^+$ and $A^1\Pi$ states are calculated. It is shown that the AlF molecule has high diagonal Franck–Condon factors ($f_{00} = 0.9949$ and $f_{11} = 0.9854$) and large Einstein coefficients for the transition of $A^1\Pi(v' = 0) \leftrightarrow X^1\Sigma^+(v'' = 0)$. In addition, the radiative lifetimes of the vibrational levels are close to 10^{-9} s for the $A^1\Pi$ state. The line intensities of the $A^1\Pi(v' = 4-15) \leftrightarrow X^1\Sigma^+(v'' = 0)$ transitions are also calculated. The calculated TDMs and transition probabilities in this work are credible and provide some guidance for the study of similar transitions, particularly for exploring interstellar space.

Keywords: potential energy curve, spectroscopic constants, radiative lifetime, Franck–Condon factors

PACS: 31.10.+z, 31.15.A–, 31.15.aj, 37.10.Mn **DOI:** 10.1088/1674-1056/ac3648

1. Introduction

Aluminum monofluoride (AlF) molecules can be produced in their gas phase at high temperatures. The physical conditions of celestial objects can be explored by studying their molecular spectra, and the results can be used as a basis to explore other astronomical phenomena. As an interstellar molecule, its radiation and spectral properties have attracted special attention from astrophysics researchers.

Experimentally, the first spectroscopic observation of the spectral range of 3180–4180 Å was performed by Yuasa.[1] The band spectrum was investigated by Rochester,[2] who discovered an absorption system at 2200–2400 Å. The emission spectra of $A^1\Pi$–$X^1\Sigma^+$ and $C^1\Sigma$–$A^1\Pi$ were described, and the analyses were reported by Naudé and Hugo.[3] In the same year, Rowlinson and Barrow[4] completed vibrational analyses of the $A^1\Pi$–$X^1\Sigma^+$ system at 2190–2360 Å and $^3\Sigma$–$^3\Pi$ system at 3450–3720 Å. Subsequently, Barrow and Rowlinson[5] examined the absorption spectrum from 1250 Å to 2000 Å, found six new singlet band systems, and discovered four excited states during the emission process of transitions to the lowest excited singlet state $A^1\Pi$. Naudé and Hugo[6] studied four new band systems of the emission spectrum for $D^1\Delta$–$A^1\Pi$, $F^1\Delta$–$A^1\Pi$, $G^1\Sigma$–$A^1\Pi$, and $F^1\Pi$–$B^1\Sigma$ and conducted vibrational and rotational analyses of the 0–0 and 0–1 bands for the $D^1\Delta$–$A^1\Pi$ system. Then, vibrational analyses of the three triplet systems $b^3\Sigma$–$a^3\Pi$, $c^3\Delta$–$a^3\Pi$, and $b^3\Sigma$–$a^3\Pi$ were performed by Dodsworth and Barrow.[7] Naudé and Hugo[8] performed rotational analyses of the 0–0, 0–1, 0–2, 1–3 bands of the $B^1\Sigma^+ \leftrightarrow X^1\Sigma^+$ system, the 0–0, 1–3, 1–4 bands of the $C^1\prod \leftrightarrow X^1\sum^+$ system, and the accurate T_e values of the $A^1\Pi$, $B^1\Sigma^+$, $C^1\prod^+$, $D^1\Delta$ states; then, they calculated the rotational and vibrational constants of the $X^1\Sigma^+$ and $B^1\Sigma^+$ states. Yoshimine and McLean[9] reported calculations of the total molecular energies, dissociation energies, and electric dipole moments for the ground states of AlF. The emission spectrum of $a^3\Pi$–$X^1\Sigma^+$ was measured by Rosenwaks *et al.*[10] Kopp *et al.*[11] reported the rotational analysis of the $A^3\Pi$–$X^1\Sigma^+$ absorption spectra using a King furnace. Murty[12] calculated the intensity factors of the $C^1\Sigma^+$–$A^1\Pi$ transition bands of the AlF molecule, and the lines of the (0,0) band of the C–A system in sunspot spectra were suggested to be restudied. Maki and Lovas[13] measured the high-resolution diode laser spectrum of AlF and studied the transitions of AlF for the 1–0, 2–1, and 3–2 bands. Hedderich and Bernath[14] extended the observation range to 5–4 bands using a Fourier transform spectrometer.

In theory, So and Richards *et al.* made *ab initio* Hartree–Fock calculations toward some states of AlF, such as $X^1\Sigma^+$, $A^1\Pi$, $D^1\Delta$ etc.[15] Murty[12] discussed the calculation of FC factors, which are crucial to the exploration of the electronic transition moment. Joshi *et al.*[16] evaluated the Franck–Condon factors (FCFs) of the A–X system. Klein and Rosmus[17] calculated the electric dipole moment functions and radiative transition probabilities of the $X^1\Sigma^+$ states of AlF using highly correlated coupled electron pair approximation (CEPA) electronic wave functions. Hirst[18] presented the PECs of the AlF relative to ground-state atoms. Langhoff *et*

[†]Corresponding author. E-mail: zygsr2010@163.com
[‡]Corresponding author. E-mail: xjgo@xupt.edu.cn

© 2022 Chinese Physical Society and IOP Publishing Ltd

al.[19] studied the PECs of $X^1\Sigma^+$ and $A^1\Pi$ of AlF and obtained the precise spectrum constants of the lowest six singlets and the lowest five triplet states of AlF. The radiative lifetimes of the excited states and Einstein coefficients of the $A^1\Pi$–$X^1\Sigma^+$ transition were also computed. Kumar *et al.*[20] evaluated the FCFs and *r*-centroids using a numerical integration procedure for the systems of $B^1\Sigma^+$–$X^1\Sigma^+$, $C^1\Sigma^+$–$X^1\Sigma^+$, $c^3\Sigma^+$–$b^3\Sigma^+$, $f^3\Pi$–$b^3\Sigma^+$, $F^1\Pi$–$B^1\Sigma^+$, and $G^1\Sigma^+$–$B^1\Sigma^+$, which made the results more convincing. They also reported the FCFs and *r*-centroids for the states of $D^1\Delta$, $E^1\Pi$, $F^1\Pi$, and the $G^1\Sigma^+$–$A^1\Pi$ transition system of the AlF molecule in the same year. Luo *et al.*[21] calculated the PECs and the values of R_e, D_e, ω_e, $\omega_e\chi_e$, B_e, and α_e of the $X^1\Sigma^+$, $A^1\Pi$, and $B^1\Sigma^+$ states using the SAC/D95(d) method. Zhao *et al.*[22] calculated the PECs, molecular parameters, and spectroscopic properties of the $X^1\Sigma^+$ state according to coupled-cluster method with single, double, and perturbative triple excitations [CCSD(T)] and Quadratic configuration interaction with single, double, and perturbative triple substitutions [QCISD(T)]. Using the MRCI method, Wells and Lane[23] studied the PECs and spectroscopic constants of the $X^1\Sigma^+$, $a^3\Pi$, $A^1\Pi$, $b^3\Sigma^+$, $B^1\Sigma^+$, $c^3\Sigma^+$, $C^1\Sigma^+$ states and the permanent dipole moments (PDMs) of the $X^1\Sigma^+$ state. With these PECs, they computed the FCFs of the $A^1\Pi \leftrightarrow X^1\Sigma^+$ and $a^3\Pi$–$X^1\Sigma^+$ transitions. Balachandrakumar *et al.*[24] evaluated the FCFs and *r*-centroid of the $C^1\Sigma^+$–$A^1\Sigma^+$, $b^3\Sigma^+$–$a^3\Pi_r$, $c^3\Sigma$–$a^3\Pi_r$, and $f^3\Pi$–$a^3\Pi_r$ band systems by applying a numerical integration procedure with suitable potential energy curves. Yousefi and Bernath[25] prepared vibration-rotation line lists of the ground electronic states ($X^1\Sigma^+$) for AlF. The potential energy surface (PES) was calculated by direct potential fitting using the rotational and rotational vibration lines of the experiment. The ro-vibrational energy levels were studied with PES.

Herein, we calculated the PECs of the $X^1\Sigma^+$ and $A^1\Pi$ states of the AlF molecule applying the complete active space self-consistent field (CASSCF) method and the MRCI approach while simultaneously considering the Davidson correction and the scalar relativity correction of the third-order DKH Hamiltonian approximation. We will briefly introduce the methodologies in our work. The PECs of the $X^1\Sigma^+$ and $A^1\Pi$ states and the TDMs of the $A^1\Pi \leftrightarrow X^1\Sigma^+$ transition are shown in Section 3. By combining PECs and TDMs, we determined the FCFs, vibrational levels and all spontaneous emission Einstein coefficients. We also computed the radiative lifetimes of the vibrational levels of the $A^1\Pi$ state. Finally, the important contents of this work are summarized. The obtained spectroscopic constants, vibrational levels and Einstein coefficients are convincing and can supply available information to measure emissions, such as those in stellar atmospheres.

2. Theory and method

The ground states of the Al and F atoms are ^3P_u and ^3P_u, respectively. The first dissociation asymptote of the AlF molecule is $^3P_u + {}^3P_u$, where the $X^1\Sigma^+$ and $A^1\Pi$ states belong to the dissociation channel. All calculations are completed in the MOLPRO 2015 package[26] in the point group. Herein, the CASSCF[27,28] is used as the reference wave function for the MRCI calculation. The AWCV5Z basis set was chosen for which it can well consider core–valence correlation effect, we studied the PECs of the two states. The calculation method of TDMs is identical.

Because of the limitation of the MOLPRO program, the symmetry of the subgroup in the point group was used in our calculations. The symmetry contains four irreducible representations: a_1, b_1, b_2, and a_2. While a_1 produces the Σ^+ state and a component of the Δ state, b_1 and b_2 supply the Π state; a_2 generates the Σ^- state and the other components of the Δ state. For the calculation of CASSCF, eight molecular orbitals (MOs) are opted as an active space ($5\sigma 6\sigma 2\pi_x 2\pi_y 7\sigma 3\pi_x 3\pi_y 8\sigma$), including the $3s^2 3p^1$ shell of Al and $2s^2 2p^5$ shell of F. The other ten electrons are distributed in the active space of a (4, 2, 2, 0), while the $1s^2 2s^2 2p^6$ orbital of aluminum is a closed-shell orbit and occupies double space. In the process of MRCI+Q,[29–31] there are 22 electrons in total during the relevant energy calculations. We selected the AWCV5Z basis set for calculations. At the same time, the scalar relativistic effect is considered through the third-order DKH Hamiltonian calculation.

The PECs were reported in previous work[23] with the CASSCF method and the MRCI+Q approach, and the AVQZ basis set was selected. The molecular orbitals (MOs) to calculate MRCI are derived from the CASSCF results. In this paper, with the AWCV5Z basis set, the eight outermost ($4a_1$, $2b_1$, $2b_2$, and $0a_2$) MOs are put into the active space. AlF has 22 electrons in total, and 10 valence electrons are divided into eight valence MOs. Therefore, the active space can be represented as CAS (10, 8). The remaining 12 inner electrons in the AlF radical are placed in the six lowest MOs ($4a_1$, $1b_1$, $1b_2$, and $0a_2$). In total, 384 external MOs ($138a_1$, $94b_1$, $94b_2$, and $58a_2$) are obtained by the MRCI calculation of PECs using the AWCV5Z basis set.

The Einstein spontaneous emission coefficient $A_{v'v''}$ from the initial level (v', J') to the final level (v'', J'') can be calculated by the following formula:[32]

$$A_{v'v''} = 3.1361891 \times 10^{-7} \frac{S(J', J'')}{2J'+1} \nu^3 \langle \psi_{v',J'} | M(r) | \psi_{v'',J''} \rangle. \quad (1)$$

Here, $A_{v'v''}$ is the Einstein spontaneous emission coefficient in units of s^{-1}; ν is the emission frequency in units of cm^{-1}; $M(r)$ is the dipole moment in units of Debye; $S(J', J'')$ is the Hönl–London rotational intensity factor; $\psi_{v',J'}$ and $\psi_{v'',J''}$ are the normalized radial wave functions.

Since the upper and lower vibrational levels can be expressed as v' and v'', the total transition probability of a certain upper level v' is gained by summing the Einstein coefficients of emissions from this upper level to all possible lower vibrational levels. The radiative lifetime of a certain upper level is determined as the reciprocal of the total transition probability, i.e.,

$$\tau_{v'} = 1 \Big/ \sum_{v''} A_{v'v''}. \tag{2}$$

Here, $A_{v'v''}$ is the Einstein coefficient of spontaneous emission from level v' to level v''; $\tau_{v'}$ is the radiative lifetime of the level v'.

The Einstein coefficient $A_{v'v''}$ of spontaneous emission is used to calculate the line intensity $I_{v'v''}$,

$$I_{v'v''} = \frac{(2J'+1)\exp\left(-\frac{hcE_{v''J''}}{kT}\right)}{8\pi c\nu^2 Q} \times A_{v'v''}. \tag{3}$$

Here, J' is the rotational level for the upper state of the absorption transition, $I_{v'v''}$ is the line intensities in units of $\mathrm{cm}^{-1}/(\mathrm{molecule}\cdot\mathrm{cm}^{-2})$, $E_{v''J''}$ is the lower-state energy of the transition in units of cm^{-1}, and T is the temperature in K. Planck's constant is $h = 6.626 \times 10^{-34}$ J·s, the light speed is $c = 3.0 \times 10^{10}$ cm/s, and Boltzmann constant is $k = 1.381 \times 10^{-23}$ J/K.

There is a positive correlation between line intensity and FCFs. Generally, the formula for calculating FCFs is

$$f_{v'v''} = |\langle \Psi_{v'J'} | \Psi_{v''J''} \rangle|. \tag{4}$$

The PECs of AlF are studied over internuclear distances of 0.8–6.8 Å. To make the results more convincing, the interval value is shortened to 0.01 Å around the equilibrium bond distance. Depending on the acquired PECs, we obtain the spectroscopic constants of the individual electronic states by solving the Schrödinger equation using the LEVEL 8.2 program,[32] which involves the equilibrium internuclear distance (R_e), harmonic frequency (ω_e), first anharmonicities ($\omega_e\chi_e$), rotational constants (B_e), depth well (D_e) and adiabatic relative electronic energy associated with the ground state (T_e).

3. Results and discussion

In this section, we first explored the PECs and spectroscopic constants of the two states through the MRCI+Q approach with the AWCV5Z basis set. Second, based on the calculated potential energy curve, the vibrational energy levels and rotational constants of the two electronic states are calculated using the level 8.2 program.[32] The transition properties are eventually studied, including PDMs, TDMs, FCFs, and radiative lifetimes. We also computed the line intensities.

3.1. PECs and spectroscopic parameters

Using the MRCI+Q approach, we selected the AWCV5Z basis set to calculate PECs and obtained the spectral constants of the two states. The PECs of the $X^1\Sigma^+$ and $A^1\Pi$ states are shown in Fig. 1. The dissociation limit of the two states is $Al(^3P_u) + F(^3P_u)$, and the internuclear distance corresponding to PECs is 0.8–6.8 Å. In addition, Table 1 lists the spectrum parameters and available experimental values of the $X^1\Sigma^+$ and $A^1\Pi$ states. For convenience, only some experimental[14,33] and theoretical[25] spectroscopic constants are listed for comparison.

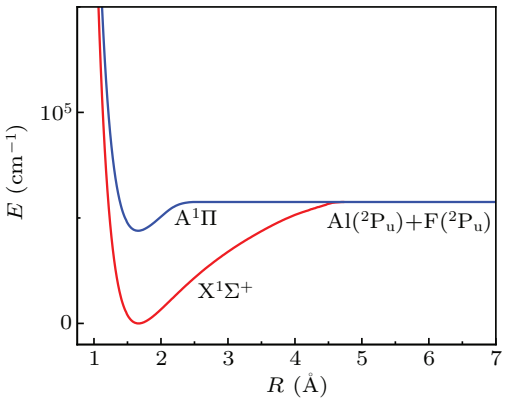


Fig. 1. PECs of the $X^1\Sigma^+$ and $A^1\Pi$ states.

Table 1. Spectroscopic constants of the $X^1\Sigma^+$ and $A^1\Pi$ states.

States	T_e (cm^{-1})	R_e (Å)	ω_e (cm^{-1})	$\omega_e\chi_e$ (cm^{-1})	B_e (cm^{-1})	D_e (eV)	References
$X^1\Sigma^+$	0	1.6644	796.1084	4.4500	0.5459	7.0357	this work
	0	1.6544	802.26	4.77	0.5524	–	experiment[33]
	–	1.6544	802.32	4.849	0.5525	–	experiment[14]
	–	1.6536	806.3542	4.7237	0.5530	–	calculation[25]
$A^1\Pi$	43915.1752	1.6579	804.2493	5.5890	0.5501	1.5908	this work
	43949.2	1.6485	803.94	5.99	0.5564	–	experiment[33]
	44211	1.664	828	–	0.5601	–	calculation[23]

There is a potential well depth of 56745.9669 cm^{-1} in the $X^1\Sigma^+$ state and 12830.7917 cm^{-1} in the $A^1\Pi$ state. Moreover, the equilibrium distance R_e between the two states is very small. According to Table 1, we calculated the spectroscopic constants of the two bound states of AlF via the AWCV5Z basis and selected the MRCI+Q level method. The previously obtained theoretical methods[25] and experimental[14,33] results are also listed for comparison. In terms of the ground

state $X^1\Sigma^+$, the calculated value of R_e is 1.6644 Å, which is 0.01 Å different from the value of 1.6544 Å, with a percentage error of only 0.6008%.[14,33] The acquired dissociation energy D_e is 7.0357 eV, and the dissociation energy has no comparable value. Our calculated B_e value is slightly smaller than the experimental result recorded by Huber *et al.*[33] However, our values have a relatively large error compared with the calculation results of Yousefi and Bernath.[25]

For the $A^1\Pi$ state, the equilibrium distance R_e is 1.6579 Å, as reported by us, which is only 0.0094 Å different from the experimental value.[33] Comparing the values of T_e, ω_e, and B_e to the results of the experimental values, we observe that the percentage errors are only 0.0775%, 0.0385%, and 1.1453%, respectively. Obviously, our values are close to the experimental results[33] and consistent with previous studies.[23] Overall, the acquired spectroscopic constants for the $X^1\Sigma^+$ and $A^1\Pi$ states of the AlF molecule are consistent with the experimental results and other available theoretical results.

According to the calculated PECs, the LEVEL 8.2 program was used to calculate the vibrational levels of the $X^1\Sigma^+$ and $A^1\Pi$ states. The digits of the vibrational levels of the $X^1\Sigma^+$ and $A^1\Pi$ states are 135 and 21, respectively (Table 2). Langhoff *et al.*[19] calculated the first nine vibrational energy levels of the $X^1\Sigma^+$ state and the $A^1\Pi$ state, and the results are also listed in Table 2. Compared with it, the difference of state $X^1\Sigma^+$ is only 0.17%–0.44%; the difference of state $A^1\Pi$ is 2.42%–4.41%. Balachandrakumar *et al.*[24] reported the first eight vibrational energy levels of state $A^1\Pi$, and their results differed by less than 1% from our calculations. Obviously, our results are close to other available theoretical results.

Table 2. Vibrational levels (cm^{-1}) of the $X^1\Sigma^+$ and $A^1\Pi$ states.

v	$X^1\Sigma^+$			$A^1\Pi$			
	G_v		B_v	G_v			B_v
	Present	Ref. [19]		Present	Ref. [19]	Ref. [24]	
0	395.2544	394.6	0.5434	399.6307	389.6	400.47	0.5475
1	1182.2979	1180	0.5385	1191.1925	1162.4	1192.26	0.5423
2	1960.0671	1956.1	0.5337	1971.6088	1920.8	1971.63	0.5371
3	2728.7522	2722.3	0.5289	2741.0496	2266.4	2738.27	0.5318
4	3488.5562	3480.2	0.5241	3499.8200	3399.3	3491.88	0.5265
5	4239.7894	4229.9	0.5192	4248.2939	4118.7	4232.15	0.5211
6	4982.7104	4970	0.5144	4986.6843	4822.1	4958.8	0.5157
7	5717.3004	5700	0.5098	5714.7724	5508	5671.52	0.5104
8	6443.2172	6419.6	0.5053	6431.7535	6174.9	6370	0.5054
9	7159.8961	7128.7	0.5012	7136.3734	6821.5		0.5007
10	7866.8399		0.4973	7827.3333			0.4960
11	8564.0980		0.4935	8503.7663			0.4909
12	9252.5363		0.4894	9165.2644			0.4850
13	9933.5128		0.4849	9811.0862			0.4778
14	10608.1166		0.4801	10438.9987			0.4695
15	11276.5783		0.4755	11044.6464			0.4600
16	11938.2972		0.4712	11621.9878			0.4491
17	12592.3999		0.4673	12164.3095			0.4364
18	13238.3952		0.4636	12664.1098			0.4207
19	13876.5164		0.4598	13110.6935			0.3997
20	14507.5501		0.4556	13484.1890			0.3658
Total	135			21			

3.2. PDMs and TDMs

The PDMs of the two states are explored with the changes in internuclear distance R at the level of MRCI+Q. The internuclear distance R of the PDMs is 1.0–6.8 Å. The PDMs of the $X^1\Sigma^+$ and $A^1\Pi$ states at R_e are −0.42476308 a.u. and −0.58900765 a.u., respectively. The PDM curves of the ground state and low excited state have approximately identical trends (Fig. 2). The PDM function of the $A^1\Pi$ state rapidly decreases from the highest value of 0.3073363 a.u. to the lowest value of −0.86346557 a.u. and eventually close to zero. The PDM function of the $X^1\Sigma^+$ state has a maximum value of 0.51201672 a.u. at 1.0 Å, falls to the minimum value of −3.15460982 a.u. at 3.3 Å, and finally becomes zero. The PDMs of the $X^1\Sigma^+$ state have a very deep potential well, which is much deeper than the state of $A^1\Pi$.

The TDMs of the $A^1\Pi \leftrightarrow X^1\Sigma^+$ transition are very close to the results of previous reports.[23] The TMD unit is distinct from the one in the previous study.[23] $X^1\Sigma^+$ and $A^1\Pi$ states have many vibrational states. As shown in Fig. 3, the internuclear distance R of TDMs is also 1.0–6.8 Å. The TDM function of the transition gradually decreases from the high-

est 1.9683034 a.u. at 1.0 Å to zero. The TDMs of the $A^1\Pi \leftrightarrow X^1\Sigma^+$ transition is 1.76300482 a.u. at R_e of the $X^1\Sigma^+$ state. Furthermore, the TDMs tend to zero when the internuclear distance R_e is approximately 4.0 Å, which is caused by the orbit-forbidden transition.

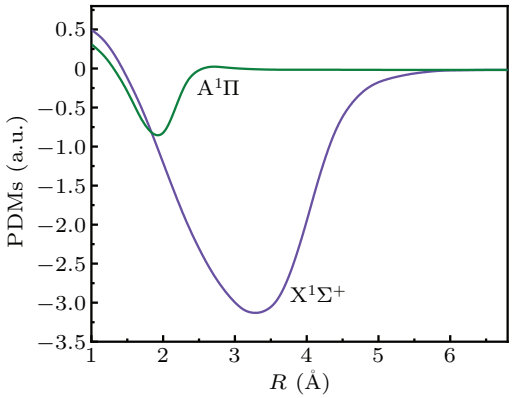


Fig. 2. PDMs of the $X^1\Sigma^+$ and $A^1\Pi$ states.

The leading electronic transition between $A^1\Pi$ and $X^1\Sigma^+$ states is the $7\sigma^2$–$7\sigma 3\pi$ promotion. According to Fig. 3, the TDMs of the $A^1\Pi \leftrightarrow X^1\Sigma^+$ transition are large near the internuclear equilibrium separations of the $A^1\Pi$ and $X^1\Sigma^+$ states. In addition, R_e of the $A^1\Pi$ state is 1.6579 Å, and R_e of the $X^1\Sigma^+$ is 1.6644 Å. Obviously, the difference between them is small. Moreover, the two states have similar PECs, and both states have deep wells. Combining with the obtained calculations, we can speculate that the emissions of the $A^1\Pi \leftrightarrow X^1\Sigma^+$ system should be substantial, and some of these emissions should be very intense based on the FC principle.

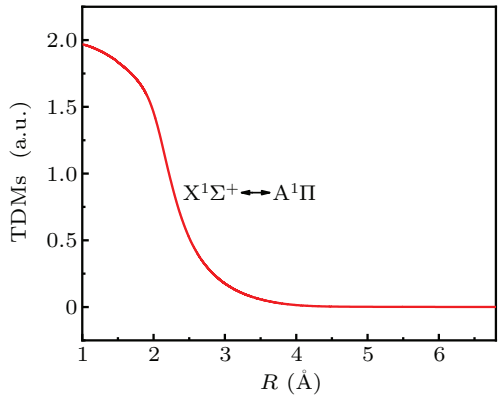


Fig. 3. TDMs for $A^1\Pi \leftrightarrow X^1\Sigma^+$.

3.3. Einstein coefficients and radiative lifetimes of $A^1\Pi \leftrightarrow X^1\Sigma^+$

Using the LEVEL 8.2 program, we calculated the FCFs and Einstein coefficients (vibrational transition probabilities) for the $A^1\Pi \leftrightarrow X^1\Sigma^+$ system in combination with the TDM function. To more clearly analyze problems, we collected several large Einstein coefficients and their FCFs, as shown in Table 3. Joshi *et al.*[16] evaluated the FCFs of the $A^1\Pi(v'=0-5) \leftrightarrow X^1\Sigma^+(v''=0-5)$ transition. After comparison, the difference is very small, such as the percentage difference of 0–0, 1–1, 2–2 and other bands is less than 0.3%, and most of the results are less than 2.6%.

Table 3. FCFs (1st line) and Einstein coefficients (s^{-1}, 2nd line) of emissions for the $A^1\Pi \leftrightarrow X^1\Sigma^+$ system.

$v'-v''$	FCFs		$A_{v'v''}$		$v'-v''$	FCFs	$A_{v'v''}$
	Present	Ref. [19]	Present	Ref. [24]		Present	Present
0–0	0.9949	0.9925	5.2805×10^8	5.2930×10^8	10–10	0.9780	4.5027×10^8
0–1	0.0051	0.004427	3.5318×10^6		11–10	0.0059	3.3180×10^4
1–1	0.9854	0.9836	5.1851×10^8	5.2342×10^8	11–11	0.9811	4.4128×10^8
2–2	0.9777	0.975	5.0953×10^8	5.1670×10^8	11–13	0.0075	2.5139×10^6
2–3	0.01220	0.01252	8.9494×10^6		12–12	0.9819	4.3014×10^8
3–2	0.01294	0.01329	4.4315×10^6	1.5350×10^6	12–14	0.0103	3.0795×10^6
3–3	0.9719	0.9665	5.0112×10^8	5.0897×10^8	13–13	0.9757	4.1499×10^8
4–3	0.0154	0.01754	4.9411×10^6	3.2817×10^6	13–15	0.0150	3.9230×10^6
4–4	0.9680	0.9583	4.9326×10^8	4.9924×10^8	14–14	0.9527	3.9239×10^8
4–5	0.0151	0.01963	1.2010×10^7		14–16	0.0232	5.2945×10^6
5–4	0.0168	0.02171	4.9465×10^6	6.4045×10^6	15–14	0.0180	2.2782×10^7
5–5	0.9662	0.9503	4.8589×10^8	4.8674×10^8	15–15	0.8950	3.5667×10^8
6–5	0.0170		4.4906×10^6	1.1750×10^7	15–16	0.0291	3.6081×10^5
6–6	0.9662		4.7890×10^8	4.7002×10^8	15–17	0.0382	7.6292×10^6
6–7	0.0139		1.2773×10^7	3.3875×10^6			
7–6	0.0163		3.6670×10^6	2.0431×10^7			
7–7	0.9679		4.7210×10^8	4.4710×10^8			
8–7	0.0146		2.6232×10^6	3.3981×10^7			
8–8	0.9708		4.6526×10^8	4.1550×10^8			
9–8	0.0122		1.5367×10^6	5.4042×10^7			
9–9	0.9743		4.5809×10^8	3.7247×10^8			

Obviously, the larger Einstein coefficients are mainly concentrated in the Frank–Condon region with a maximum value of 5.2805×10^{8} s^{-1} (Table 3), which corresponds to the strong transition $v'=0\rightarrow v''=0$. For the emissions from the states of $A^1\Pi(v'=0-9)$ to $X^1\Sigma^+(v''=0-12)$, the largest Einstein coefficient is 5.293×10^{8} s^{-1}, as studied by Langhoff *et al.*,[19] which is consistent with our value, and the error is only 0.237%. In this study, the obtained Einstein coefficients are compared with those given by Langhoff *et al.*,[19] It can be seen that the results in the Frank–Condon region are basically the same, the difference is 0.18%–5.6%, but the results in other bands are quite different. This may be due to different choices of the calculation method and basis set.

Based on the obtained Einstein coefficients, we computed the radiative lifetimes of all vibrational levels of $A^1\Pi$. In this work, all Einstein coefficients are used for radiative lifetime calculations. For the convenience of discussion, the results are listed in Table 4. As observed from the list, the spontaneous radiative lifetimes of all vibrational levels are approximately 10^{-9} s. Our results are consistent with those of Langhoff *et al.*,[19] and the radiative lifetimes increase with increasing vibration levels. Based on the available results, all radiative lifetimes of the $A^1\Pi$ states are short, which implies that the radiation of the $A^1\Pi\leftrightarrow X^1\Sigma^+$ system should be stable.

Table 4. Radiative lifetimes (ns) for the vibrational levels ($v'=0$–15 of the $A^1\Pi$ state.

	This work	Calculation[19]
0	1.8810	1.89
1	1.8970	1.91
2	1.9148	1.93
3	1.9346	1.96
4	1.9566	1.99
5	1.9814	2.02
6	2.0090	2.05
7	2.0396	2.09
8	2.0735	2.14
9	2.1110	2.19
10	2.1534	
11	2.2026	
12	2.2616	
13	2.3336	
14	2.4228	
15	2.5350	

The relationship between the wavenumber and the absolute line intensities of $A^1\Pi\leftrightarrow X^1\Sigma^+$ is shown in Fig. 4. The line intensities of the $A^1\Pi(v'=4-15)\leftrightarrow X^1\Sigma^+(v''=0)$ transitions are calculated according to Einstein coefficients. For the transition, the calculated results are classified into R and P branches up to at 296 K. Because the order of the magnitude of $v'=0\rightarrow v''=0$ band transitions is larger than those of other bands, the trend of the absolute line intensities and the wavenumber cannot be seen in the plot. In terms of the transition bands of $v''=0\rightarrow v'=4$–15, the absolute line intensities first increase and subsequently decrease with the wavenumber (Fig. 4). In fact, for the bands of $v''=0\rightarrow v'=0$–15, the wavenumber is first at 43918.4624 cm^{-1} (P(1)) with the maximum line intensity of 9.8572×10^{-17} cm^{-1}/(molecule·cm^{-2}), and it decreases to the minimum value at the band of $v''=0\rightarrow v'=0$–4. The wavenumber is at 46998.2962 cm^{-1} (P(16)) with the line intensity of 3.3014×10^{-27} cm^{-1}/(molecule·cm^{-2}); then, the transition intensity increases to the $v''=0\rightarrow v'=5$ band. The wavenumber is at 47767.1191 cm^{-1} (P(1)) with the line intensity of 3.5462×10^{-26} cm^{-1}/(molecule·cm^{-2}), subsequently decreases to the minimum value at the band of $v''=0\rightarrow v'=6$ with the intensity of 2.6996×10^{-28} cm^{-1}/(molecule·cm^{-2}) and slightly rises to the maximum value at the band of $v''=0\rightarrow v'=9$. The wavenumber is at 50655.2122 cm^{-1} (P(1)) with the line intensity of 9.4111×10^{-27} cm^{-1}/(molecule·cm^{-2}) and finally decreases. The results show that the band of $v''=0\rightarrow v'=0$ is the strongest excitation for the $A^1\Pi\leftrightarrow X^1\Sigma^+$ system. The maximum line intensity is located in the 0–0 band, and the line intensity is 9.8572×10^{-17} cm^{-1}/(molecule·cm^{-2}) at 47767.1191 cm^{-1} (P(1)).

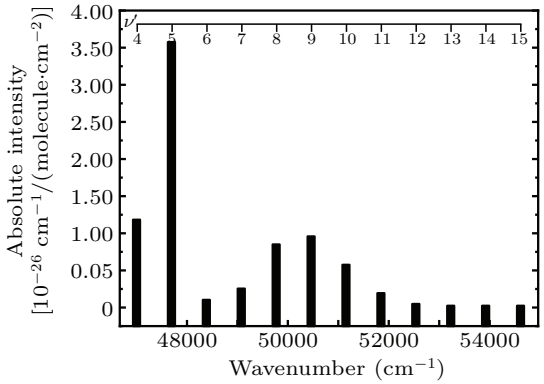


Fig. 4. Absolute intensities of the $v''=0\rightarrow v'=4-15$ transition bands of the $A^1\Pi\leftrightarrow X^1\Sigma^+$ system.

4. Conclusions

In general, according to the CASSCF/MRCI+Q approach and (4,2,2,0) active space, we have theoretically calculated the PECs, spectroscopic constants, PDMs, TDMs, and vibrational levels of the $X^1\Sigma^+$ and $A^1\Pi$ states of AlF. Also, we have computed the line intensities of the $A^1\Pi(v'=4-15)\leftrightarrow X^1\Sigma^+(v''=0)$ transitions. The maximum line intensity is located in the 0–0 band, and the line intensity is 9.8572×10^{-17} cm^{-1}/(molecule·cm^{-2}) with a position of 47767.1191 cm^{-1} (P(1)). The spectroscopic constants of the $X^1\Sigma^+$ and $A^1\Pi$ states can be acquired by solving the radial Schrödinger equation using the LEVEL 8.2 program. In contrast, our results are very close to the previous results.[14,33] According to these achieved values, we obtain the FCFs ($f_{00}=0.9949$) of the $A^1\Pi\leftrightarrow X^1\Sigma^+$ transition. In

addition, for the $X^1\Sigma^+(v'=0) \leftrightarrow A^1\Pi(v''=0)$ system, the emission is strong, and the strong radiation spectrum is mainly concentrated in the ultraviolet range. The radiative lifetimes of the vibrational levels of the $A^1\Pi$ state are approximately. Furthermore, the lifetime is short for the lower vibrational levels, but it rapidly increases with the increase in vibrational levels.

Acknowledgements

This work was supported by the National Natural Science Foundation of China (Grant No. 11947127) and the Shaanxi Natural Science Foundation, China (Grant No. 2018JM1053).

References

[1] Yuasa T 1938 *Science Reports of the Tokyo Bunrika Daigaku, Section A* (Tokyo: Editorial Committee of Tsukuba Journal of Mathematics) pp. 239–248
[2] Rochester G D 1939 *Phys. Rev.* **56** 307
[3] Naudé S and Hugo T 1953 *Can. J. Phys.* **31** 1106
[4] Rowlinson H C and Barrow R F 1953 *Proc. Phys. Soc. A* **66** 437
[5] Barrow R F and Rowlinson H C 1954 *Proc. R. Soc. London A* **224** 134
[6] Naudé S and Hugo T 1954 *Can. J. Phys.* **32** 246
[7] Dodsworth P and Barrow R 1955 *Proc. Phys. Soc. A* **68** 824
[8] Naudé S and Hugo T 1957 *Can. J. Phys.* **35** 64
[9] Yoshimine M and Mclean A D 1967 *Int. J. Quantum Chem.* **1** 313
[10] Rosenwaks S, Steele R E and Broida H P 1976 *Chem. Phys. Lett.* **38** 121
[11] Kopp I, Lindgren B and Malmberg C 1976 *Phys. Scr.* **14** 170
[12] Murty P 1977 *Solar Phys.* **54** 377
[13] Maki A and Lovas F 1982 *J. Mol. Spectrosc.* **95** 80
[14] Hedderich H G and Bernath P F 1992 *J. Mol. Spectrosc.* **153** 73
[15] So S and Richards W 1974 *J. Phys. B: Atom. Mol. Phys.* **7** 1973
[16] Joshi G C, Joshi U C, Punetha L M and Pande M C 1982 *Bull. Astr. Soc. India* **10** 159
[17] Klein R and Rosmus P 1984 *Theoret. Chim. Acta* **66** 21
[18] Hirst D M 1987 *J. Mol. Spectrosc.* **121** 189
[19] Langhoff S R, Bauschlicher Jr C W and Taylor P R 1988 *J. Chem. Phys.* **88** 5715
[20] Kumar K B, Rajamanickam N, Bagare S, Gomez M F and Gonzalez J L 2003 *Astropart. Phys.* **20** 67
[21] Luo W L, Mao J W, Wu D L, Zhou L L and Xie A D 2006 *J. At. Mol. Phys.* **3** 427 (in Chinese)
[22] Zhao J, Zeng H and Zhu Z 2011 *Comput. Theor. Chem.* **963** 130
[23] Wells N and Lane I C 2011 *Phys. Chem. Chem. Phys.* **13** 19018
[24] Balachandrakumar K, Raja V, Karthikeyan B, Bagare S P and Rajamanickam N 2015 *Adv. Astron.* **2015** 846840
[25] Yousefi M and Bernath P F 2018 *Astrophys. J. Suppl. S* **237** 8
[26] Werner H, Knowles P, Knizia G, Manby F, Schütz M, Celani P, Györffy W, Kats D, Korona T and Lindh R 2015 *Molpro Quantum Chemistry Software* http://www.molpro.net [2021-09-30]
[27] Werner H J and Knowles P J 1985 *J. Chem. Phys.* **82** 5053
[28] Knowles P J and Werner H J 1985 *Chem. Phys. Lett.* **115** 259
[29] Langhoff S R and Davidson E R 1974 *Int. J. Quantum Chem.* **8** 61
[30] Werner H J and Knowles P J 1988 *J. Chem. Phys.* **89** 5853
[31] Knowles P J and Werner H J 1988 *Chem. Phys. Lett.* **145** 514
[32] Le Roy R J 2017 *J. Quant. Spectrosc. Radiat. Transfer* **186** 167
[33] Huber K P 2013 *Molecular spectra and molecular structure: IV Constants of diatomic molecules* (New York: Springer Science & Business Media) pp. 20–23